



Numerical Analysis of the Effect of Cavity Location on Settlement Behavior

Esraa Fakhri Ahmed^a and Moataz A. Al-Obaydi*

^a Department of Civil Engineering, College of Engineering, University of Mosul, Mosul, Iraq

*Corresponding author E-mail: dralobaydi@uomosul.edu.iq

Abstract

Structures founded on the soil mass encounter stability issues due to cavity that may naturally forms in soluble soil or rock. A significant risk associated with excessive settlement and a reduction in strength of soil. The coupled behavior of soil, foundation, and structure subjected to seismic loading in the presence of cavities is investigated using 3D-PLAXIS software based on FEM. The study examined the impact of cavity positions on foundation settlement and building deflection. The horizontal distance from foundation center to center of cavity (X) was expressed as a ratio to foundation width (B) ($X/B=0, 0.5, 1$ and 2), while depth of cavity was expressed as a ratio between vertical distance between foundation base and cavity crown (H) to foundation width (B) of ($H/B= 0.067, 0.2, 0.4, 0.8, 1.33$ and 2). The results indicated that in case of no-cavity, the settlement increased considerably to 142 mm under seismic load compared to 62 mm under static load, and the differential settlement increased from zero to 11 mm due to seismic load. The risk condition arose when the cavity found under foundation's edge ($X/B=0.5$). The maximum total and differential settlements under seismic load were 148 mm and 38 mm, which were 4.05% and 245.5% more than in event of no-cavity. Under the limitations of the current study, the influence of cavity on settlement diminished when the cavity offset to location ($X \geq B$) and the effective depth of cavity extended to ($H=0.8B$). The maximum building floor deflection exhibited when a cavity positioned beneath foundation ($X/B=0$).

Keywords: Dynamic load, inter-storey drift, building deflection, Cavity, total settlement, differential settlement.

1. Introduction

Cavities are significant subsurface features that influence the soil behavior particularly under the seismic load. When the cavity existing in the soil mass causes a substantial differential settlement of foundation [1,2]. The differential settlement induced by cavities forms cracking within building walls and roofs [3]. There is a critical zone beneath the foundation, when cavity is located outside this zone, it has no apparent impact [4-6]. Only when locates within the foundation's failure zone can poses an impact [7-9].

Many studies considered the influence of cavity under the static load condition [10-13]. Al-Tabbaa et al. [14] indicated that a shallow cavity located close a strip foundation is the most risk case. And the cavity with a circular shape is less critical than the square one. Wang et al. [15] found the size and location of cavity have effect on the bearing capacity. Using finite element software PLAXIS 2D, Lee et al. [16] found that the bearing capacity factor of square cavities increased with increased their horizontal and vertical distance from the foundation. But the capacity factor remained constant when the cavity located outside the critical zone. Hussein and Snodi [17] examined the effect of square cavity on the bearing capacity of a square foundation located on a gypseous soil using Plaxis 3D program. The cavity effect vanished when located at depth $4B$ to $6B$. The influence of cavity diminishes when the horizontal distance is $X=1.5B$ and the vertical distance between the foundation and the cavity is $H=3B$ [18]. The cavity location and load eccentricity have a significant impact on



This is an open access article under the terms of the Creative Commons Attribution License, which permits use, distribution and reproduction in any medium, provided the original work is properly cited. © 2025 The Authors

<https://www.muthuni-ojs.org/index.php/mjet/index>

the bearing capacity, where the bearing capacity increases with increasing the distance between the crown of cavity and the underneath of foundation to $H=2B$ and then the cavity effect vanishes [19,20]. The displacement increases as the cavity approach foundation and as increases in the size of cavity, which it may collapse with reduces the distance between cavity and the foundation or size of cavity [21]. There is a critical zone when the cavity is outside that zone, then, no effect on the foundation's stability or bearing capacity [22]. The size and type of failure zone were found to vary with the cavity depth, cavity offset, shear strength factor. Still, the failure mechanism is not significantly impacted by the form of the foundation [23].

On the other hand, the cavity may act as a barrier against the propagation of seismic waves which reflects or refracts. This is resulting an amplification of ground motion due to high concentrated of seismic energy around the cavity [24]. Pokhrel and Kuwano [25] experimentally investigated the issue of earthquake on cavity stability by a number of shaking table tests. Zhang et al. [26] numerically studied the seismic bearing capacity of undrained clay containing a single, continuous square void considering the cavity depth, cavity offset, cavity size and undrained shear strength. It was found that increasing in the depth of cavity (H) and horizontal distance (X) led to increase the seismic bearing capacity while reduced with size of cavity. The factor of safety reduced with decreasing the cavity depth and increasing cavity size, and the collapse occurred under high peak ground acceleration for various cavity depth 2-10m, depending on the cavity size [27]. Xiao et al. [28] examined the seismic bearing capacity of a strip foundations placed on a cohesive-frictional soil with existence of square cavities, using an adaptive finite element limit analysis. The minimum seismic bearing capacity achieved when the cavity was located at the edge of foundation. The critical zone varied inversely with the value of horizontal coefficient of acceleration. Previous studies demonstrated that the presence of cavities in the soil mass poses a high risk to structures and their stability. Most of them examined the effect of cavities on the settlement and bearing capacity of soil under the static load. Limited studies have considered the behavior of cavity under the seismic load. However, to understanding the actual behavior of soil-foundation-structure interaction in presence of cavity, it is reliable to consider the mechanism of the complex system interaction. Therefore, a numerical analysis carried out using the PLAXIS 3D software to evaluate the influence of cavity on the behavior of soil-foundation-building system under a dynamic load in terms of settlement, differential settlement, deform and inter-storey of building.

2. Material Properties and Numerical Modelling

2.1. Geometry of the problem

The problem under the study is a site involves a site consisting of clay soil bounded by dimensions of $150 \times 150 \times 100$ m. The structure is a 15-story building has an area of 12×12 m and 45 m height, founded on a raft foundation of area 15×15 m. A cavity of cubic shape exists in the soil mass at different locations relative to the axis of building foundation.

2.2. Soil properties

The proposed $C-\phi$ soil has been considered as a soil under the foundation. The properties of the soil are presented in Table 1. The Hardening Soil model with small-strain stiffness (HS-small strain) was selected to simulate the behavior of the soil under the static and dynamic loading.

Table 1: The properties of the soil adopted in the study

Parameter	Symbol	Unit	Value
Material Model	Model	---	HS small
Type	---	---	Drained
Unsaturated unit weight	γ_{unsat}	kN/m^3	17
Saturated unit weight	γ_{sat}	kN/m^3	18
Secant stiffness in standard drained triaxial test	E_{50}^{ref}	kN/m^2	20000
Tangent stiffness for primary oedometer loading	$E_{\text{rand}}^{\text{ref}}$	kN/m^2	20000
Unloading / reloading stiffness	$E_{\text{ur}}^{\text{ref}}$	kN/m^2	60000
Cohesion	c'_{ref}	kN/m^2	14
Angle of internal friction	ϕ'	degree	24
Angle of dilatancy	ψ	degree	0
Power for stress-level dependency of stiffness	m	---	0.7
Poisson's ratio for unloading-reloading	ν_{ur}	---	0.25
Reference shear modulus at very small strains	G_0^{ref}	kN/m^2	75000
Threshold shear strain at which $G_s = 0.722G_0$	$\gamma_{0.7}$	---	2×10^{-4}

Shear wave velocity	V_s	m/sec	210
Shear strength reduction	R_{int}	---	0.75
Mass coefficient	α	---	0.2474
Stiffness coefficient	β	---	7.579E-3

2.3. Foundation properties

The raft foundation was chosen in this study, with dimensions (15 m × 15 m) with a thickness of 1.5 m. The properties of concrete foundation are unit weight of 25 kN/m³, Modulus of elasticity of 28600 MPa, Poisson's ratio 0.15 behaved as elastic.

2.4. Cavity shape and size

The cubic cavity has dimensions of (3.75 × 3.75 × 3.75) m. Accordingly, the ratio of length of cubic cavity to the width of foundation (L/B) was 0.25.

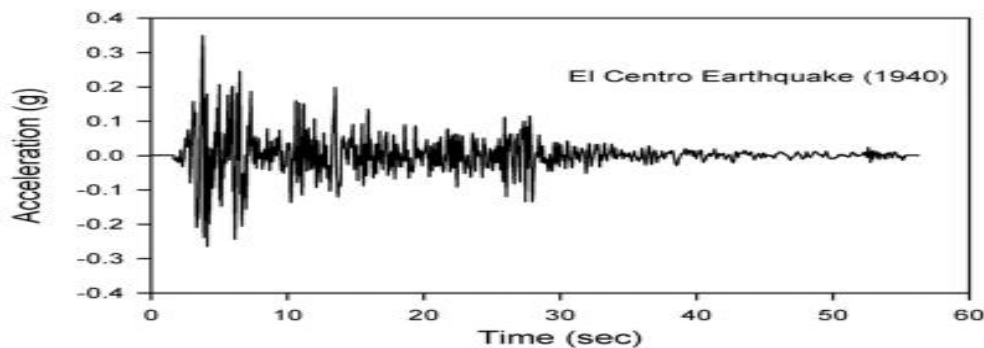
2.5. Cavity locations

Different vertical distances (depths) of the cubic cavity were adopted. The depths are (1, 3, 6, 12, 20, and 30) m. These depths considered as a ratio of H/B, where H is the depth of cavity from the footing base to the cavity crown, and B is the width of footing. The ratios H/B are (0.067, 0.2, 0.4, 0.8, 1.33, and 2).

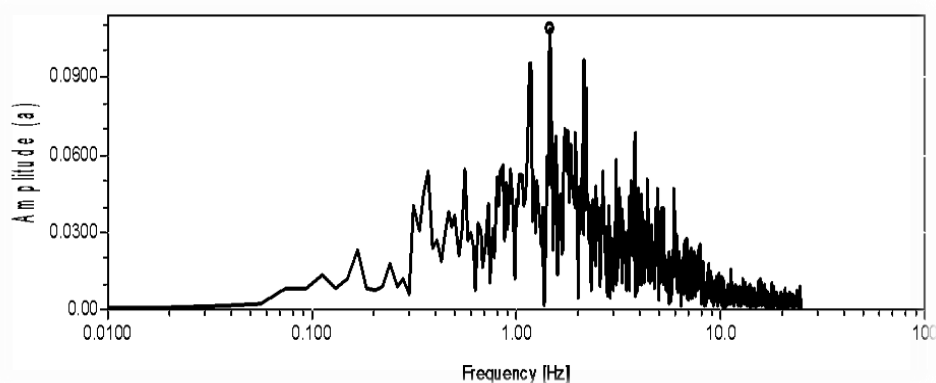
Several horizontal distances were taken into account, which are (0, 7.5, 15, and 30) m. These distances were taken as a ratio, represented by X/B, where X it is the horizontal distance between the center of the cavity to the center of the footing and B is the width of the foundation. The X/B ratios are (0, 0.5, 1, and 2).

2.6. Ground motion characteristics

For dynamic analysis, the selection of input motion is based on the acceleration time history records of earthquakes. In this study, the far-field acceleration record of the El-Centro 1940 earthquake has a peak ground acceleration of 0.349g have been selected, as illustrated in Fig. 1a [29]. A wide range of input motion with predominant and maximum frequencies are 1.5Hz and 4Hz respectively as shown in Fig 1b.



(a) Far field acceleration record



(b) The Fourier spectrum

Fig. 1: El-Centro 1940 earthquake characteristics [29]

2.7. Numerical simulation

To model the cavity, foundation and building, the PLAXIS 3D software based on the finite element method has been used to simulate 15 stories building rested on raft foundation. The 10-node tetrahedral element has been selected to simulate the soil media, while a plate element was used to model the foundation and slabs of building. Beam elements were used to model the beams and columns of the building.

The behavior of soil-structure interaction is simulated using 12-node interface elements (PLAXIS 3D, 2020). A static load corresponding to building load and seismic load represented by El-Centro earthquake were applied.

The finite element mesh presented in Fig. 2 which has dimensions of 150×150×100 m. The type of fine mesh was used in modeling to ensure the accurate results. Regarding the boundary conditions for static and dynamic problems, it was employed free field boundaries at the lateral boundaries whereas a compliant base introduced at the bottom of the soil medium.

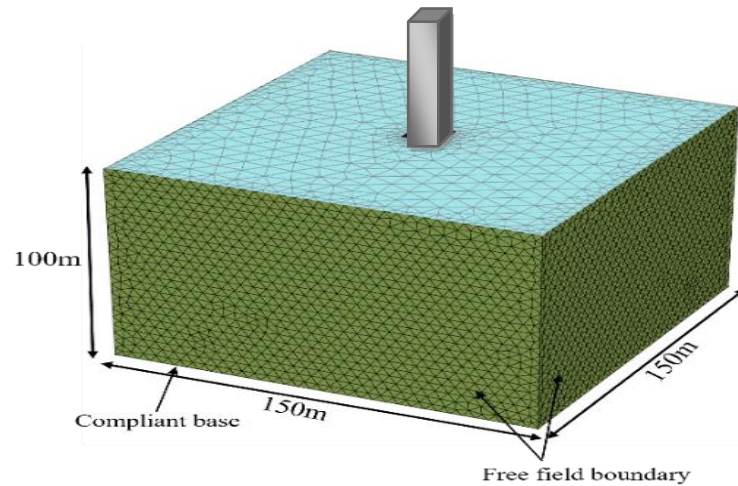


Fig. 2: The finite element mesh and boundary condition of the model

2.8. Modeling validation

To examine the modeling followed in the present study using Finite Element software (PLAXIS 3D), a verification was carried out with the model proposed by Xu and Fatahi [30] that used a Finite Difference software (FLAC 3D). They performed a dynamic analysis on a building with 15 stories found on soft soil and subjected to El Centro earthquake.

The results obtained from the present study and those obtained by Xu and Fatahi [30] are presented in Fig. 3. It seems that a good comparable result of the both studies regarding the horizontal displacement of the building. The current study achieved less displacement by 13.35%.

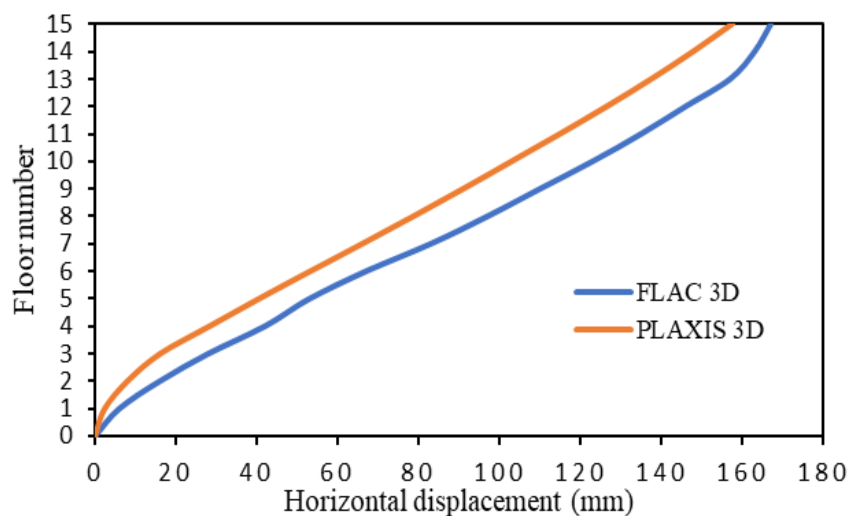


Fig. 3: The horizontal displacement using FLAC 3D [30] and PLAXIS 3D (current study).

3. Results and Discussion

3.1. Effect of cubic cavity on the settlement

Figure 4 shows variations of settlement (δ_s) with different locations of cavity. The δ_s decreases with the increasing depth of cavity (H) and with distance (X). The cubic cavity with a size of ($L/B = 0.25$) displays a slight effect on δ_s . The settlement varies between 135 mm to 148 mm with ± 6 mm compared to 142 mm exhibits in case of no-cavity. Cavity sites at ($X/B = 0$ and 0.5) shows further impact on the settlement than the distances ($X/B=1$ and 2). When the cavity locates outside the effective region of external load, then the settlement values drop below that of no-cavity case. The effective depth of cavity concerning the δ_s is ($H/B = 0.2$). The maximum δ_s of 147mm and 148mm recorded at $X/B = 0$ and 0.5 respectively. Consequently, the cubic cavity of size ($L/B = 0.25$) does not pose a threat under the seismic load. Regarding the settlement results and under the circumstances of the present study, the critical zone of such cavity limited by ($X < B$) and ($H < 1.33B$). Previous studies [19,31] show that effect of cavity diminished at depth more than $2B$, while other found that the ineffective depth of square cavity is $4B$ to $6B$ [17].

The impact of seismic load appeared through increases the δ_s from 62 mm (static) to 148 mm (dynamic) about twice, for most cavity locations. The high stresses concentrate at the corner of cubic cavity as well as at the region between the cavity and foundation that leads to increase in the settlement when cavity locates within the critical zone near the foundation. Under static load condition, the stress concentrated under the foundation when cavity locates in critical zone [5]. In addition, the shallow cavity amplifies the seismic waves that caused a more concentrated in stresses and hence more settlement than the static condition. Lancioni et al. [32] also reported that the wave is magnified when cavity near the ground surface. Comparison of settlement values from the current study and those allowable, it obvious that the static settlement is fall within the permissible settlement of clay soil (65-100) mm for raft foundation [33], however, the settlement achieved under seismic load exceeds the 100 mm.

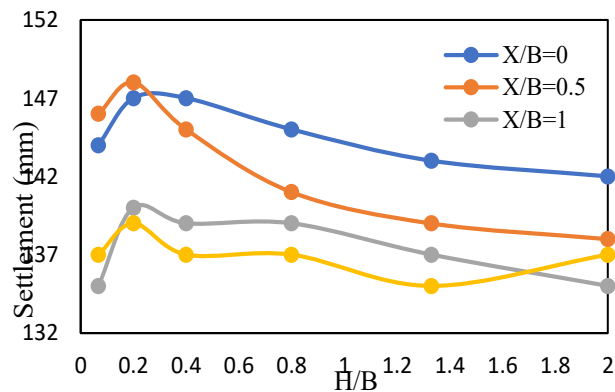


Fig. 4: Effect of cavity location on the settlement

3.2. Effect of cubic cavity on the differential settlement

The relationship between cavity locations on the differential settlement (δ_d) is shown in Fig. 5. The nonlinear response of soil to seismic load is the cause of variations in the δ_d , in addition, to the response of cavity to seismic waves that may decrease the overall soil bearing. When cavity locates at ($X/B = 0.5$) and depth ($H/B = 0.067, 0.2$, and 0.4) shows maximum settlements of (38, 35, and 21) mm respectively, by (245, 218, and 91) % increasing over no-cavity case. These increases in δ_d attributed to concentrate of stresses at the edge of foundation and to seismic waves amplify by the cavity. This result is consistent with that of Xiao et al. [28], who found that the cavity positioning under the edge of foundation gives a lowest seismic bearing capacity. Smaller values of δ_d exhibits when the cavity located at ($X/B = 0$). Cavity moves away from the foundation displays a lower δ_d varies between 7mm to 17mm.

Consequently, it can be stated that the high risk of cavity when it's located at shallow depths under the foundation edge. This because of a high stress achieves at the edge of foundation particularly under seismic load which rises the differential settlement from 11mm (for static) to 38mm (for dynamic) about 3.5 times increases. Accordingly, the critical zone bounds by ($X < B$) and ($H < 0.8B$) considering the study restrictions. The differential settlements under static and dynamic loads does not exceeding the permissible limits of 40 mm [33].

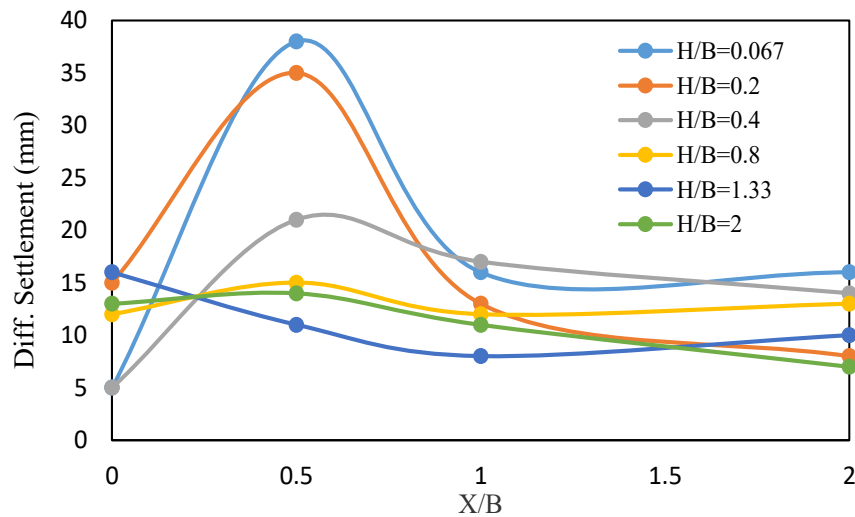


Fig. 5: Effect of cavity location on the differential settlement

3.3. Deformation pattern of soil

The presence of cavity within the soil mass as a discontinuity is altering in deformation values especially under the foundation and around the cavity as presented in Table 2. The variation in pattern of deformation with cavity depth (H) for the case of cavity locates under the centerline of foundation ($X/B=0$) is illustrated in Fig. 6. For the shallow cavity ($H/B=0.067$), a high vertical displacement initiates in the region between the cavity crown and the foundation base of order 168 mm and 144 mm at the cavity crown and under the foundation respectively. The vertical displacement reduces with the cavity depth to maximum values (174, 140 and 116) mm recorded at the crown of cavity for ($H/B=0.2, 0.4$ and 0.8) respectively. Nevertheless, the deeper cavities have slight influence on the deformation.

On the other hand, Fig. 7 shows the deformation pattern for the case of cavity locates at the edge of foundation ($X/B=0.5$). Again, about similar behavior exhibits as in the case of ($X/B=0$), unless high values of vertical deformation achieve at the edge of foundation as well as at the crown of cavity. The maximum displacements recorded at the edge of foundation are (146, 148, 145, 141, 139 and 138) mm for ($H/B=0.067, 0.2, 0.4, 0.8, 1.33$ and 2) respectively.

Furthermore, Fig. 8 describes the effect of horizontal position of cavity (X) on the deformation pattern when cavity locates at shallow depth ($H/B=0.067$). For the cavity locates under the center of foundation ($X/B=0$), approximately a uniform deformation attains under the foundation with a maximum value reaches 168 mm. It increases to a value of 195 mm when the cavity locates under the edge of foundation ($X/B=0.5$), which causes a high differential settlement due to the non-uniform stress distribution. Moreover, an increase in the offset of cavity to ($X/B=1$), the vertical displacement unaffected by the cavity and so on for ($X/B=2$). Similarly for cavity depth ($H/B=0.2$), Fig. 9 shows that the deformation pattern influences when the cavity near the foundation at ($X/B=0$ and 0.5), beyond the ($X/B=0.5$) the displacement under the foundation unaffected by the presence cavity.

Table 2: Maximum vertical deformation under the base of foundation and at crown of cavity

Depth of cavity (H/B)	Vertical deformation (mm)							
	Offset of cavity (X/B)							
	0		0.5		1		2	
	At base of foundation	At cavity crown	At base of foundation	At cavity crown	At base of foundation	At cavity crown	At base of Foundation	At cavity crown
0.067	144	168	146	195	135	112	137	50
0.2	147	174	148	197	140	75	139	45
0.4	147	140	145	170	139	70	137	49
0.8	145	116	141	89	139	70	137	53
1.33	143	76	139	80	137	53	135	63
2	142	56	138	55	130	54	137	50

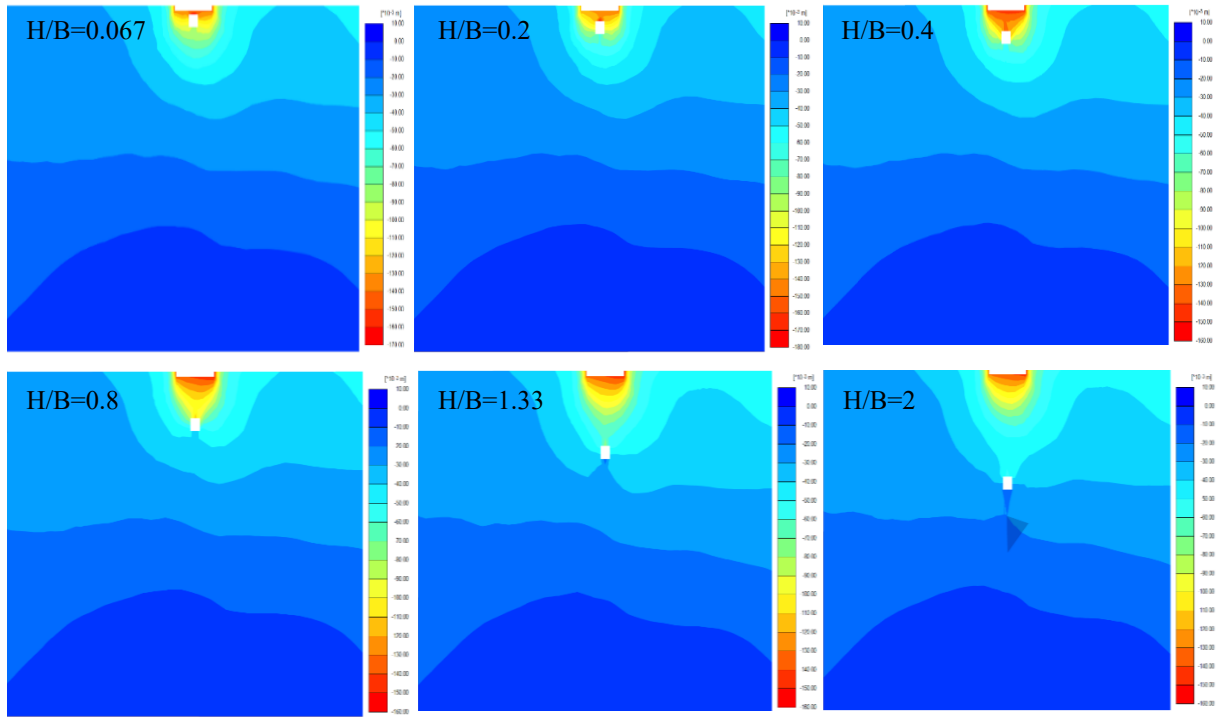


Fig. 6: Pattern of vertical deformation with cavity depth when $X/B = 0$

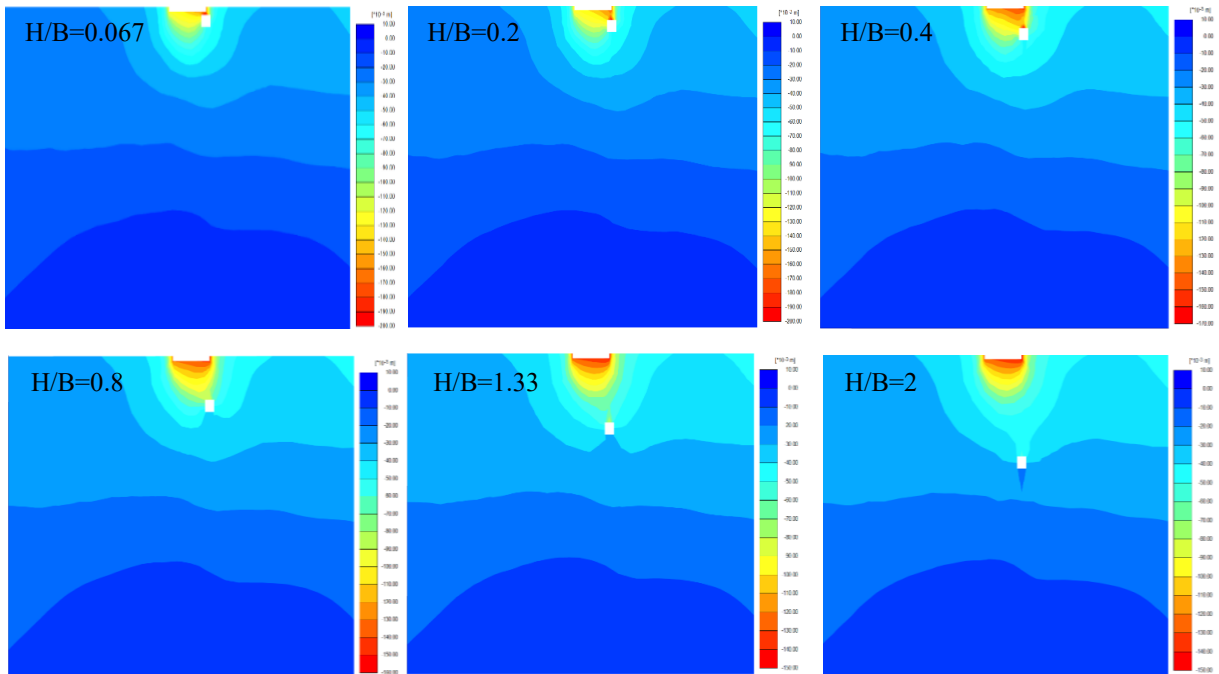


Fig. 7: Pattern of vertical deformation with cavity depth when $X/B = 0.5$

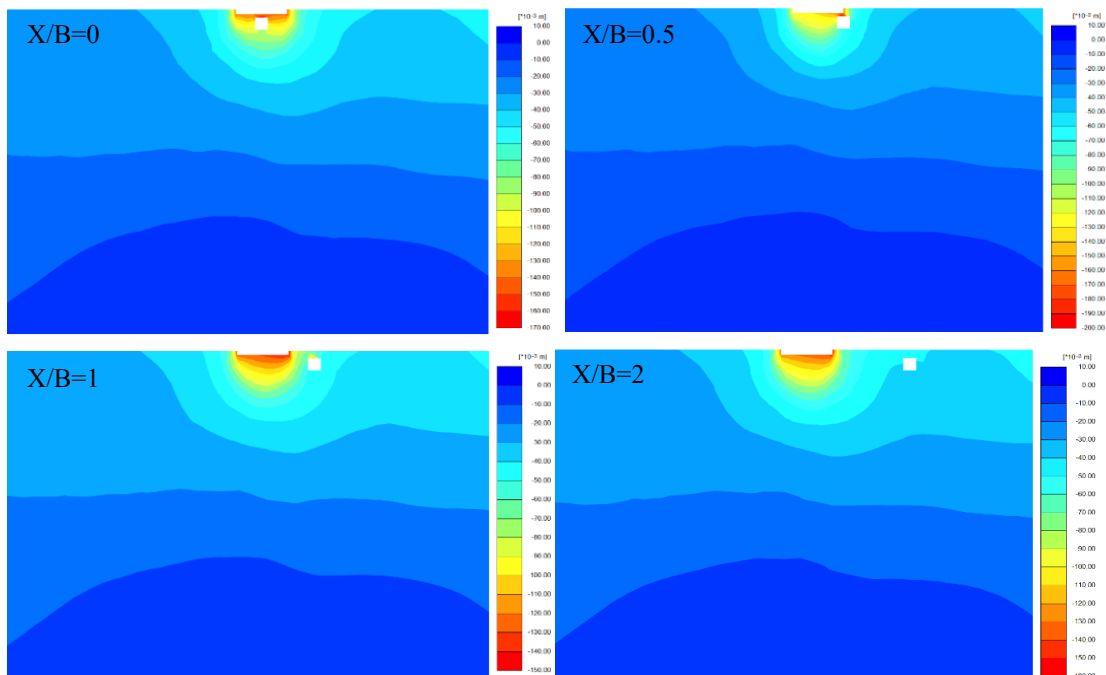


Fig. 8: Pattern of vertical deformation with cavity offset when $H/B = 0.067$

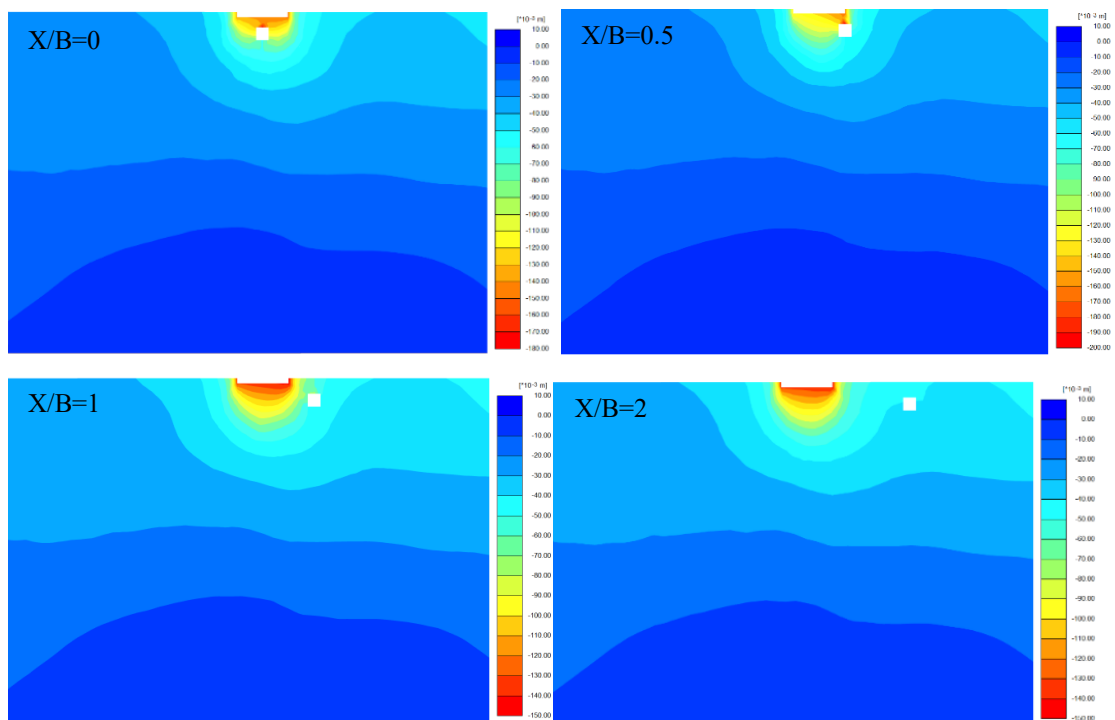


Fig. 9: Pattern of vertical deformation with cavity offset when $H/B = 0.2$

3.4. Building deflection

The deflection of building was measured through the horizontal displacement of the floors. Figure 10a shows that the horizontal displacement of upper floor reaches 139 mm when cavity locates at the edge of foundation ($X/B=0.5$). At further distance ($X/B=1$ and 2), the displacement decreases to about 50% as the cavity offset away from the active zone of external load. In addition, the impact of the cavity due to the seismic wave magnification is insignificant on the building for far cavity. When cavity sites at ($X/B=0$), the displacement reduces to 36 mm which is less than the case without cavity. Regarding the inter-storey drift (IDR), Fig. 10b indicates a maximum value of 0.31% for the case of ($X/B=0.5; H/B=0.067$). The value of IDR drops to 0.16% when cavity sites at ($X/B=1$ and 2) which is approximately approach the value 0.13% of the case without cavity. This is because the cavity is located outside the critical zone. Cavity at distance ($X/B=0$) exhibits lower IDR value of 0.09% which is less than the value without cavity. In all cases the value of inter-storey drift not exceeded the allowable limit of 1.5% that proposed by *Australian standard for concrete structure AS 3600* [34]. Al-Farham et al. [35] stated that the horizontal displacement and inter-storey drift increases as the tunnel approach the structure.

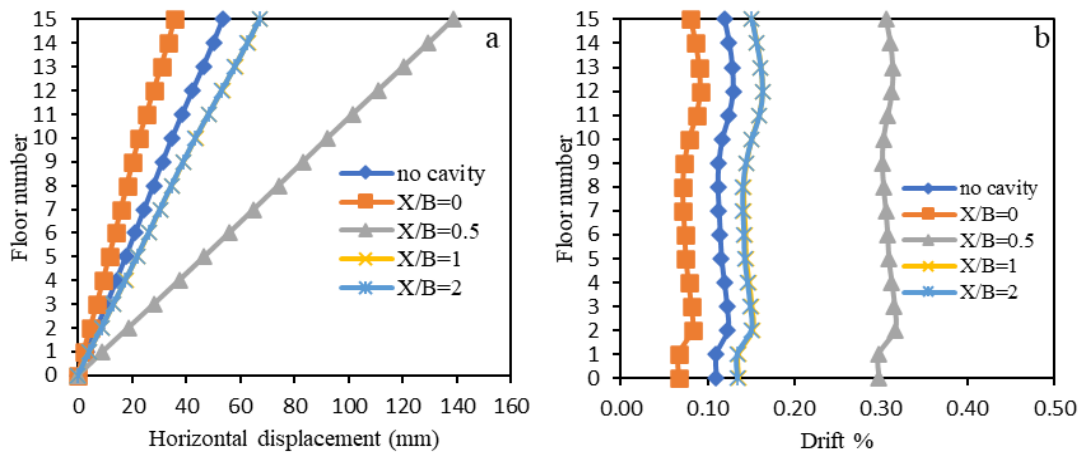


Fig. 10: Effect of cubic cavity location horizontally at ($H/B=0.067$)
a) horizontal displacement, b) inter-storey drift.

4. Conclusions

The following conclusions can be drawn under the limitations of the study as soil type, static and dynamic loads intensity, size and shape of cavity:

1. In case of no-cavity, the settlement under the static load is 62 mm which increases to 142 mm due seismic load. Additionally, the differential settlement increases from zero to 11 mm.
2. There is a critical zone forms under the building foundation represents the region of the impact of cavity. Such zone is defined as ($X < B$, $H < 1.33B$) depends on total settlement, while for differential settlement the zone became narrow ($X \leq 0.4B$, $H \leq B$).
3. The most critical case happened when the cavity was sited under the edge of foundation ($X/B = 0.5$).
4. A cavity located at ($X/B = 0.5$) produces a maximum settlement of 148 mm and a maximum differential settlement of 38 mm under the seismic load. The total settlement is approximately the same as that of the no-cavity case, while the differential settlement is 245.5% higher than in the case of no-cavity.
5. Generally, the effect of cavity vanishes when the cavity is offset far from foundation ($X \geq B$).
6. The presence of cavity changed the deformation pattern, with increases detected at the edge of foundation as well as at the crown of the cavity.
7. The maximum deflection and inter-storey drift of the building were exhibited when cavity was located at the edge of foundation ($X/B=0$).
8. The conclusions presented above are limited by the scope of this study. These limitations include cavity size and shape, soil properties, and intensity of applied loads (static and dynamic). Therefore, it is recommended that these limitations be considered in future studies due to their importance

References

- [1] Baus RL & Wang MC (1983), Bearing capacity of strip footing above void. *The Journal of Geotechnical Engineering* 109(1), 1–14.
- [2] Wu G, Zhao M, Zhang R & Liang G (2020), Ultimate bearing capacity of eccentrically loaded strip footings above voids in rock masses. *Computers and Geotechnics* 128, 103819. <https://doi.org/10.1016/j.compgeo.2020.103819>
- [3] Al-Jazaairry A & Sabbagh T (2017a), Effect of cavities on the behaviour of strip footing subjected to inclined load. *International Journal of Civil, Environmental, Structural, Construction and Architectural Engineering* 11(3), 255-261.
- [4] Peng FL, Kiyosumi M, Ohuchi M & Kusakabe O (2006), Cavity effects on the bearing capacity of footing foundations and the calculation method. Proceeding GeoShanghai 2006, *In Underground Construction and Ground Movement*, 50–57. [https://doi.org/10.1061/40867\(199\)4](https://doi.org/10.1061/40867(199)4)
- [5] Khalil A & Khattab S (2009), Effect of cavity on Stress distribution and Settlement under Foundation. *Al-Rafidain Engineering Journal* 17(6), 14-29.
- [6] Mazouz B, Mansouri T, Baazouzi M & Abbeche K (2022), Assessing the effect of underground void on strip footing sitting on a reinforced sand slope with numerical modeling. *Engineering, Technology and Applied Science Research* 12(4), 9005–9011. <https://doi.org/10.48084/etasr.5131>
- [7] Roby AS & Leander T (2022), Analysis of cavities on performance of shallow footing: a review. *International Journal of Engineering Research & Technology (IJERT)* 10(6), 78-70. <https://doi.org/10.17577/IJERTCONV10IS06023>
- [8] Chaabani W, Remadna MS & Abu-Farsakh M (2023), Numerical modeling of the ultimate bearing capacity of strip footings on reinforced sand layer overlying clay with voids. *Infrastructures* 8(1). <https://doi.org/10.3390/infrastructures8010003>

- [9] Mofidi-Rouchi J & Nozari MA (2023), Effect of twin circular underground voids on bearing capacity of strip foundations. *European Journal of Engineering Science and Technology*, 6(2), 1–13. <https://doi.org/10.33422/ejest.v6i2.1137>
- [10] Pusadkar SS, Harne SS & Thakare SW (2017), Performance of strip footing above multiple square voids in C-Ø soil. *International Journal of Engineering Research & Technology (IJERT)*, 6(6).
- [11] Sabouni R & Airan M (2018), Evaluation of foundation on soil with cavities: a case study from the UAE. *International Journal of Structural and Civil Engineering Research* 7(4), 358–363. <https://doi.org/10.18178/ijscer.7.4.358-363>
- [12] Mazouz, B., Mansouri, T., Baazouzi, M., & Abbeche, K. (2022). Assessing the Effect of Underground Void on Strip Footing Sitting on a Reinforced Sand Slope with Numerical Modeling. *Engineering, Technology and Applied Science Research*, 12(4), 9005–9011. <https://doi.org/10.48084/ctasr.5131>
- [13] Al-Jazaairry A & Sabbagh T (2017b), Effect of cavities on the behaviour of model pile under axial loading in sand. *Proceeding of the World Congress on Civil, Structural, and Environmental Engineering* 2(4), 1-10. <https://doi.org/10.11159/icgre17.107>
- [14] Al-Tabbaa A, Russell L & O'Reilly MP (1989), Model test of footings above shallow cavities. *Ground Engineering*, 22, 39-42.
- [15] Wang MC, Jao M & Hsieh CW (1994), Effect of underground cavity on footing interaction. *13th International Conference on Soil Mechanics and Foundation Engineering (ICSMFE, 1994)*, ISSMGE, 575-578.
- [16] Lee JK, Jeong S & Ko J (2014), Undrained stability of surface strip footings above voids. *Computers and Geotechnics*, 62, 128–135. <https://doi.org/10.1016/j.compgeo.2014.07.009>
- [17] Hussein IS & Snodi LN (2020), Effect of cavities from gypsum dissolution on bearing capacity of soil under square footing. *Key Engineering Materials* 857, 221–227. <https://doi.org/10.4028/www.scientific.net/KEM.857.221>
- [18] Saadi D, Abbeche K & Boufarh R (2020), Model experiments to assess effect of cavities on bearing capacity of two interfering superficial foundations resting on granular soil. *Studia Geotechnica et Mechanica* 42(3), 222–231. <https://doi.org/10.2478/sgem-2019-0046>
- [19] Mansouri T, Boufarh R & Saadi D (2021), Effects of underground circular void on strip footing laid on the edge of a cohesionless slope under eccentric loads. *Soils and Rocks* 44(1), 1–10. <https://doi.org/10.28927/SR.2021.055920>
- [20] Mansouri T, Benabid A, Saadi M & Benaicha AC (2022), Impact of underground cavity on a strip footing at the edge of a cohesionless slope and subjected to eccentric load. *5th International Conference of Contemporary Affairs in Architecture and Urbanism (ICCAUA-2022)*, 909–917. <https://doi.org/10.38027/iccaua2022en0090>
- [21] Taleb HA & Guemidi I (2023), Studied the impact of the foundation on the underground cavity using the finite element method. *Journal of Scientific Technology and Engineering Research* 4(1), 9–16. <https://doi.org/10.53525/jster.1232122>
- [22] Azeddine B & Abdelghani M (2023), The cavity's effect on the bearing capacity of a shallow footing in reinforced slope sand. *Soils and Rocks*, 46(1). <https://doi.org/10.28927/SR.2023.003622>
- [23] Khosravi S, Karimpour-Fard M, Shahnazari H, Aminpour M & Nazem M (2024), Undrained bearing capacity of circular and square footings above centric and eccentric three-dimensional cavities. *International Journal of Geomechanics*, 24(6). <https://doi.org/10.1061/ijgnai.gmeng-8835>
- [24] Sanò T (2011), Local seismic response in presence of subsurface cavities. *Ingegneria Sismica* 28(2), 25-34. <https://www.researchgate.net/publication/289352971>
- [25] Pokhrel P, & Kuwano J (2020), Stability of underground cavity subjected to seismic motion. *The 17th World Conference on Earthquake Engineering*, 17WCEE, Sendai, Japan.
- [26] Zhang R, Feng M, Xiao Y & Liang G (2020), Seismic Bearing Capacity for Strip Footings on Undrained Clay with Voids. *Journal of Earthquake Engineering* 26(9), 4910-4923. <https://doi.org/10.1080/13632469.2020.1851316>
- [27] Fabozzi S, de Silva F, Nocentini M, Peronace E, Bilotta E & Moscatelli M (2021), Seismic vulnerability of shallow underground cavities in soft rock. *Proceedings of the 8th ECCOMAS Thematic Conference on Computational Methods in Structural Dynamics and Earthquake Engineering (COMPdyn 2021)*, In M. Papadrakakis and M. Fragiadakis (Eds.), ECCOMAS Proceedia, 202-211. <https://doi.org/10.7712/120121.8474.18971>
- [28] Xiao Y, Zhao M & Zhang R (2023), Seismic bearing capacity for strip footings above voids in cohesive-frictional soils. *Earthquake Spectra* 39(1), 269–287. <https://doi.org/10.1177/87552930221141110>
- [29] Bagheri M, Ebadi-Jamkhaneh M & Samali B (2018), Effect of seismic soil–pile–structure interaction on mid- and high-rise steel buildings resting on a group of pile foundations. *International Journal of Geomechanics* 18(9). [https://doi.org/10.1061/\(ASCE\)GM.1943-5622.0001222](https://doi.org/10.1061/(ASCE)GM.1943-5622.0001222)
- [30] Xu R & Fatahi B (2015), Three-dimensional numerical analysis of seismic soil-structure interaction considering soil plasticity. *6th International Conference on Earthquake Geotechnical Engineering (6ICEGE)*.
- [31] Kumar P, Metya S, Shubham K. & Prashad D (2022), Behaviour of strip footing over cavity subjected to inclined and eccentric loads. *Arabian Journal of Geosciences* 15(1442). <https://doi.org/10.1007/s12517-022-10739-6>
- [32] Lancioni G, Bernetti R, Quagliarini E & Tonti L (2014), Effects of underground cavities on the frequency spectrum of seismic shear waves. *Advances in Civil Engineering* 2014 (Article ID 934284). <https://doi.org/10.1155/2014/934284>
- [33] Das BM (2007), Principles of foundation engineering. Cengage Learning, 7th Edition.
- [34] Standards Australia. (2018). *Australian standard for concrete structure AS 3600*.
- [35] Al-Farhan ZF, Al-Obaydi MA & Al-Saffar QN (2022), Tunnel-soil-structure interaction under seismic load. *Geotechnical Engineering and Sustainable Construction - Sustainable Geotechnical Engineering*, 91–102. https://doi.org/10.1007/978-981-16-6277-5_8